Natural history of Asian lineage Zika virus infection in macaques

Dawn M. Dudley[1*], Matthew T. Aliota[2*], Emma L. Mohr[3*], Andrea M. Weiler[4], Gabrielle Lehrer-Brey[4], Kim L. Weisgrau[4], Mariel S. Mohns[1], Meghan E. Breitbach[1], Mustafa N. Rasheed[1], Christina M. Newman[1], Dane D. Gellerup[4], Louise H. Moncla[1,2], Jennifer Post[4], Nancy Schultz-Darken[4], Josh A. Eudailey[5], M. Anthony Moody[5], Sallie R. Permar[5], Shelby L. O'Connor[1], Eva G. Rakasz[4], Heather A. Simmons[4], Saverio Capuano III[4], Thaddeus G. Golos[4,6], Jorge E. Osorio[2], Thomas C. Friedrich[2,4], and David H. O'Connor[1,4]

[1]Department of Pathology and Laboratory Medicine, University of Wisconsin-Madison; [2]Department of Pathobiological Sciences, University of Wisconsin-Madison;[3]Department of Pediatrics, School of Medicine and Public Health, University of Wisconsin-Madison; [4]Wisconsin National Primate Research Center, University of Wisconsin-Madison; [5]Department of Pediatrics and Human Vaccine Institute, Duke University Medical Center; [6]Department of Comparative Biosciences and Obstetrics and Gynecology, University of Wisconsin-Madison.

*These authors contributed equally to this work.

Infection with Asian lineage Zika virus has been associated with Guillain-Barré syndrome and fetal microcephaly[1-4]. Here we show that rhesus macaques are susceptible to infection by an Asian lineage Zika virus isolate that shares more than 99% nucleotide identity with strains currently circulating in the Americas. Following subcutaneous inoculation, Zika virus RNA was detected in plasma one-day post infection (dpi) in all animals (N = 3). Plasma viral loads peaked above 1 x 10^6 viral RNA copies/mL in two of three animals. Viral RNA was also present in saliva, urine, and cerebrospinal fluid (CSF), consistent with case reports from infected humans. Zika virus RNA persisted in both

plasma and urine at low levels for more than two weeks. Infection was associated with transient increases in proliferating natural killer cells, CD8+ and CD4+ T cells, and plasmablasts, suggesting pathogen sensing by the immune system. These data establish that Asian lineage Zika virus infection in rhesus macaques provides a relevant animal model for human infection. Furthermore, because fetal development is well characterized in rhesus macaques, infections in pregnant macaques will enable important studies of fetal defects associated with Zika virus.

Zika virus (ZIKV) is a mosquito-borne flavivirus first identified in 1947 that is divided into African and Asian lineages based on phylogeny and geographical origin[5]. The primary vector for ZIKV is *Aedes aegypti*, the same species that transmits dengue (DENV) and chikungunya (CHIKV) viruses[6]. Little was known about ZIKV when increased incidence of fetal microcephaly and Guillain-Barré syndrome occurred coincident with epidemic spread of Asian lineage ZIKV in South America. The virologic and immunologic parameters of ZIKV infection remain unknown, including tissue tropism, duration of infection, and the potential for persistence. To date, ZIKV RNA has been detected in plasma, urine, semen, CSF, breast milk and saliva of patients[4,7-10], but the extent to which this represents replication-competent, transmissible virus is unknown. Infectious virus has been isolated from saliva and a small number of case reports suggest that ZIKV may be transmitted by blood transfusion or sexual intercourse, but the likelihood of such non-vectored transmission remains undetermined[11-13]. These and many other questions cannot be resolved quickly by studying case reports of infected individuals alone.

We therefore sought to develop a relevant animal model to understand ZIKV pathogenesis, and to evaluate candidate vaccines and therapeutics. For decades, macaques have been used in both infectious disease and obstetric research. In fact, what is now known as the African lineage of ZIKV was initially discovered in a sentinel rhesus macaque kept in the Zika forest of Uganda for yellow fever surveillance[14]. But does the currently circulating Asian

51 lineage virus, which shares ~90% nucleotide identity with the African lineage, also infect
52 macaques[5]?
53 To determine this, we inoculated three Indian-origin rhesus macaques (*Macaca mulatta*)
54 subcutaneously with 1 x 10^6, 1 x 10^5, or 1 x 10^4 PFU ZIKV derived from a French Polynesian
55 virus isolate (Zika virus/H.sapiens-tc/FRA/2013/FrenchPolynesia-01_v1c1) (Fig. 1a). This range
56 of inocula is based on previous work in related flaviviruses such as West Nile virus (WNV) and
57 DENV, where it was estimated that mosquitoes delivered 1 x 10^4- 1x 10^6 PFU of virus[15]. DENV
58 infection of macaques also provides the precedence for using subcutaneous inoculations[16].
59 Blood was sampled daily for 11 days post-infection (dpi) and every 3-4 days thereafter. Viral
60 RNA (vRNA) was quantified by qRT-PCR[17]. Plasma viremia was detected in all three animals at
61 1 dpi and was proportional to the inoculum dose, underscoring the importance of selecting a
62 ZIKV challenge dose in macaques that approximates the dose encountered during either vector-
63 borne or sexual transmission (Fig. 1b)[8,11]. Peak plasma viremia occurred between 2 and 6 dpi,
64 and ranged from 8.2 x 10^4 to 2.5 x 10^6 vRNA copies/mL. The estimated doubling time for the
65 plasma viremia of individual animals ranged from 4.8 to 10.2 hours and appeared to be
66 independent of the infecting dose. By 10 dpi, plasma viral loads were undetectable (<100
67 copies/mL) in all three animals, although intermittent low-level detection (<550 copies/mL)
68 continued in two of three animals through 17 dpi.
69 To detect signs of morbidity, animals were evaluated daily for evidence of disease,
70 injury, or psychological abnormalities (e.g., inappetence, dehydration, diarrhea, depression,
71 inactivity, trauma, self-injurious or stereotypical behavior). All animals exhibited mild to
72 moderate inappetence, which led to mild weight loss in two animals. Two animals (912116 and
73 393422) also developed a very mild rash around the inoculation site one dpi that persisted for 4-
74 5 days. No other abnormal clinical signs were noted (e.g., increased body temperature, joint
75 pain, lymphadenopathy, lethargy).

76 To examine potential within-host evolution, we deep sequenced both the challenge stock
77 and plasma virus from each animal at 4 dpi. Like all flaviviruses, the ZIKV genome encodes a
78 single, large polyprotein that is co- and post-translationally processed into three structural
79 (envelope E, membrane precursor prM, capsid C) and seven non-structural (NS1, NS2A, NS2B,
80 NS3, NS4A, NS4B, and NS5) proteins[18]. The ZIKV challenge stock consensus sequence
81 matched the Genbank sequence (KJ776791) of the parental virus, but there were 8 sites where
82 between 5-40% of sequences contained variants (Fig. 2a). Maintenance of some of the
83 challenge stock variants, as well as de novo variants not detected in the challenge stock, were
84 noted in all three animals at 4 dpi (Fig. 2b). Variants were concentrated in the NS1, NS2A and
85 NS2B regions for the both the challenge stock and from the animals.
86 To measure how selection may be shaping the viral populations during replication in
87 macaques, we calculated measures of synonymous (πS) and nonsynonymous (πN) nucleotide
88 diversity in each coding region of the genome relative to the inoculum for each animal at 4 dpi.
89 The ratio of πS to πN can indicate how selection is acting on a gene. While most coding regions
90 revealed signatures of purifying selection, the regions encoding NS1 and NS2B exhibited
91 elevated levels of nonsynonymous diversity in all three animals (Fig. 2c). NS1 exists in multiple
92 forms, including a membrane--bound mNS1 form and a secreted sNS1 form. These forms are
93 implicated in a number of flavivirus--host interactions, including immune protection, disease
94 pathogenesis, and evasion of the complement system[19,20]. Thus, diversification in NS1 genes
95 could be the result of selective pressures imposed by the macaque host. Further study is
96 required to determine whether NS1 and NS2B are consistently under positive selection in
97 macaques, and to identify candidate selective pressures. However, our data suggest that they
98 may be good targets for future studies of ZIKV immunity and host adaptation.
99 Animals were monitored using complete blood counts and blood chemistry panels daily
100 for 11 dpi and then every 3 to 4 days thereafter (Extended Data Fig. 1). Similar to other viral
101 infections, a transient lymphopenia was observed beginning 1 dpi, reaching a nadir 4 dpi

102 (Extended Data Fig. 1f). The animal that received the highest dose of inoculum developed
103 leucocytosis at 7 dpi that persisted through 28 dpi and was characterized by a mature
104 neutrophilia. Each animal also exhibited evidence of a mild regenerative anemia characterized
105 by varying degrees of polychromasia and anisocytosis, but whether this was secondary to the
106 viral infection or simply a result of frequent blood draws could not be determined. All animals
107 developed an elevated serum creatine kinase (CK), which correlated directly with inoculum dose
108 and peaked 5 dpi (Extended Data Fig. 1). Increased CK is often noted in animals after repeated
109 sedation and venipuncture. Two of three animals also exhibited an approximate two-fold
110 increase in AST and ALT, which peaked at 5 dpi. These findings are not uncommon in acute
111 viral infections in humans. Both cellular dyscrasias and elevated transaminases have been
112 described in human ZIKV case reports; myositis has not been reported[21,22].
113 We next characterized the immune response to infection in lymphocyte subsets by
114 staining peripheral blood mononuclear cells (PBMC) for multiple lineage and activation markers.
115 Proliferating (Ki-67+) NK cells, CD8+ T cells, and CD4+ T cells expanded significantly above
116 baseline levels by 5 dpi; the most rapid increase occurred in the animal challenged with the
117 highest ZIKV dose (Fig. 3). We also enumerated circulating plasmablasts, defined as CD3-/20-
118 /14-/16-/11c-/123- and CD80+/HLA-DR+ cells, on 3, 7, 11 and 14 dpi (Fig. 3)[23]. The peak
119 plasmablast expansion was inoculum-dose-dependent by day 7 and the decline in plasmablast
120 cells was inversely related to inoculum dose. Together these data provide an estimate that peak
121 activation of the adaptive immune response and antibody production may occur 5-7 dpi and
122 depend on inoculum dose, informing future work to characterize these responses.
123 In addition to blood, several other body fluids were tested for ZIKV by qRT-PCR
124 including urine, saliva and CSF. Viruria was detected starting at 4 or 5 dpi and continued up to
125 14 dpi, in urine passively collected from cage pans (Fig. 1b). Despite possible degradation of
126 virus between the time of urination and sample collection and processing, 1×10^3-1×10^4 vRNA
127 copies/mL urine were detected at multiple timepoints. Virus was also detected in oral swabs

128 collected from all three animals, peaking at approximately 1 x 10^4 vRNA copies per sample in 2
129 of 3 animals (Fig. 1b). Notably, as with urine, the kinetics of virus detection in saliva occurred
130 after peak plasma viremia. Lumbar punctures were performed at 4 and 14 dpi to quantify viral
131 RNA in CSF; vRNA was detectable at 4 dpi in two of three animals (Fig. 1b).

132 Altogether, our study showed the persistence of ZIKV in the plasma of rhesus macaques
133 for approximately 10 days, similar to other vector-borne flaviviruses that cause acute, typically
134 self-limiting infections in humans. However, the prolonged detection of vRNA in urine and saliva
135 after apparent clearance from the blood, detection of virus in the CSF, and occasional plasma
136 "blips" after initial clearance, suggest that ZIKV could establish a more persistent infection.
137 Given reports of neurologic complications arising from ZIKV infection, the central nervous
138 system may be a reservoir site for persistent virus. Future work in rhesus macaques will seek to
139 determine whether virus from fluids other than blood can infect new hosts and what threshold of
140 viral load at these sites may be required for transmission.

141 While Asian lineage viruses are associated with fetal microcephaly or Guillain-Barré
142 syndrome, African lineage ZIKV is not, suggesting that the lineages may have important
143 biological differences. To begin to investigate this possibility, we also infected three macaques
144 with the African lineage Zika virus/R.macaque-tc/UGA/1947/MR766-3329, using the same three
145 doses as the Asian lineage infections (Extended Data Fig. 2). Although all three animals
146 became infected, viremia was only detected in two animals 1 dpi. The African lineage virus
147 achieved peak plasma levels at least one order of magnitude lower those observed in animals
148 infected with the Asian-lineage virus (Extended Data Fig. 2). This difference in *in vivo* viral
149 kinetics could be relevant for both virus transmission and pathogenesis. We are currently
150 working to complete the characterization of these infections.

151 Our study establishes the rhesus macaque as a relevant translational model for ZIKV
152 infection and pathogenesis in humans. Rhesus macaques support replication of both Asian
153 lineage and African lineage ZIKV, providing the possibility to conduct detailed comparative

154 pathogenesis studies. The large immunological toolset available for rhesus macaques will
155 enable investigations of immunity and potential vaccines. Pregnancy, the maternal-fetal
156 interface, and fetal development have been described in detail in rhesus macaques, so this
157 model will also enable assessments of the impact of maternal ZIKV infection on the developing
158 fetus.
159

160 **Methods**

161 *Study design*

162 This was a proof-of-concept study was designed to establish the infectivity and viral dynamics of
163 Asian lineage ZIKV. Because nothing is known about ZIKV dosing in macaques, one male
164 rhesus macaque of Indian ancestry was challenged with each of the following ZIKV doses:
165 $1x10^6$, $1x10^5$, and $1x10^4$ PFU ZIKV from each lineage. All macaques utilized in the study were
166 free of Macacine herpesvirus 1, Simian Retrovirus Type D, Simian T-lymphotropic virus Type 1,
167 and Simian Immunodeficiency Virus. In a follow-up study, two additional males and one female
168 macaque were infected with the African lineage ZIKV at the same three challenge doses as the
169 Asian lineage. Primary data from the study is available at goo.gl/rmNCqf.
170

171 *Care and use of macaques at the Wisconsin National Primate Research Center*

172 All macaque monkeys used in this study were cared for by the staff at the Wisconsin National
173 Primate Research Center (WNPRC) in accordance with the regulations and guidelines outlined
174 in the Animal Welfare Act and the Guide for the Care and Use of Laboratory Animals and the
175 recommendations of the Weatherall report. This study was approved by the University of
176 Wisconsin-Madison Graduate School Institutional Animal Care and Use Committee (Animal
177 Care and Use Protocol Number G005401). For all procedures (i.e., physical examination, virus
178 inoculation, blood and swab collection), animals were anesthetized with an intramuscular dose

179 of ketamine (10 mL/kg). Blood samples were obtained using a vacutainer system or needle and
180 syringe from the femoral or saphenous vein.
181
182 *Inoculations*
183 ZIKV strain H/PF/2013 (GenBank: KJ776791), originally isolated from a 51-year-old female in
184 France returning from French Polynesia with a single round of amplification on Vero cells, was
185 obtained from Xavier de Lamballerie (European Virus Archive, Marseille France). ZIKV strain
186 Zika virus/R.macaque-tc/UGA/1947/MR766-3329 (GenBank:LC002520), originally isolated from
187 a sentinel Rhesus monkey on 20 April 1947 in Zika Forest, Entebbe, Uganda with 149 suckling
188 mouse brain passages and two rounds of amplification on Vero cells, was obtained from Brandy
189 Russell (CDC, Ft. Collins, CO). Virus stocks were prepared by inoculation onto a confluent
190 monolayer of C6/36 mosquito cells. A single harvest of virus with a titer of 1.26 x 10^6 PFU/mL
191 for the Asian lineage (equivalent to 1.43 x 10^9 vRNA copies/mL) and 5.9 x 10^6 PFU/mL for the
192 African lineage was used for all three challenges of each lineage. The stock was thawed, diluted
193 in PBS to the appropriate concentration for each challenge, and loaded into a 1 mL syringe that
194 was kept on ice until challenge. Animals were anesthetized as described above, and 1 mL of
195 inocula was administered subcutaneously over the cranial dorsum. At the conclusion of the
196 procedure, animals were closely monitored by veterinary and animal care staff for adverse
197 reactions and signs of disease.
198
199 *Viral RNA isolation from plasma*
200 Fresh plasma and PBMC were isolated from EDTA-treated whole blood by Ficoll density
201 centrifugation at 1860 rcf for 30min. The plasma layer was collected and centrifuged for an
202 additional 8 min at 670 rcf to remove residual cells. RNA was extracted from 300 µl of plasma

203 using the Viral Total Nucleic Acid Purification Kit (Promega, Madison, WI) on a Maxwell 16 MDx
204 instrument. The RNA was then quantified by quantitative RT-PCR.
205
206 *Viral RNA isolation from urine*
207 Urine was collected from a pan beneath the animal's cage. Urine was centrifuged for 5 min at
208 500 rcf to remove cells and other debris. RNA was isolated from 300 µl urine using the Viral
209 Total Nucleic Acid Purification Kit (Promega, Madison, WI) on a Maxwell 16 MDx instrument.
210
211 *Viral RNA isolation from oral swabs*
212 Oral swab samples were collected from infected animals while anesthetized by gently running a
213 sterile swab under the animal's tongue. Swabs were placed immediately into either RNAlater or
214 viral transport medium (tissue culture medium 199 supplemented with 0.5% FBS and 1%
215 antibiotic/antimycotic) for 60-90 minutes. Samples were vortexed vigorously, then centrifuged
216 for 5 min at 500 rcf before removing the swabs. Samples were stored at either -20°C (RNAlater
217 samples) or -80°C (viral transport medium) until processing. Prior to extraction, virus was
218 pelleted by centrifugation for 1 hour at 4°C at 14000 rpm. Supernatant was removed, leaving the
219 virus in 200 µl media. Viral RNA was extracted from these samples using the Qiamp MinElute
220 Virus Spin kit (Qiagen, Germantown, Maryland) with all optional washes. Viral load data from
221 oral swabs are expressed as vRNA copies/mL eluate.
222
223 *Quantitative reverse transcription PCR (qRT-PCR)*
224 Viral RNA isolated from plasma, urine, or oral swabs was quantified by qRT-PCR using the
225 primers and probe designed by Lanciotti et al.[17] or using primers with a slight modification to
226 those described by Lanciotti et al. to accommodate the African lineage virus. The sequence of
227 these modified primers are as follows: forward-5'CGYTGCCCAACACAAGG-3', reverse 5'-

228 CCACYAAYGTTCTTTTGCABACAT-3', and probe 5'-6fam-
229 AGCCTACCTTGAYAAGCARTCAGACACYCAA-BHQ1-3'. The RT-PCR was performed using
230 the SuperScript III Platinum one-step quantitative RT-PCR system (Invitrogen, Carlsbad, CA) on
231 the LightCycler 480 instrument (Roche Diagnostics, Indianapolis, IN). Primers and probe were
232 used at final concentrations of 600 nm and 100 nm respectively, along with 150 ng random
233 primers (Promega, Madison, WI). Cycling conditions were as follows: 37°C for 15 min, 50°C for
234 30 min and 95°C for 2 min, followed by 50 cycles of 95°C for 15 sec and 60°C for 1 min. Virus
235 concentration was determined by interpolation onto an internal standard curve composed of
236 seven 10-fold serial dilutions of a synthetic ZIKV RNA fragment based on the Asian lineage. A
237 comparison of the crossing point detected by qRT-PCR found from the standard template, Asian
238 lineage virus and African lineage virus when using either the universal primer set developed by
239 our group, or the primers developed by Lanciotti et al., suggest that the efficiency of each primer
240 set is the same for both lineages of ZIKV (Extended Data Fig. 3).
241
242 *Viral quantification by plaque assay*
243 All ZIKV screens and titrations for virus quantification were completed by plaque assay on Vero
244 cell cultures. Duplicate wells were infected with 0.1 mL aliquots from serial 10-fold dilutions in
245 growth media and virus was adsorbed for one hour. Following incubation, the inoculum was
246 removed, and monolayers were overlaid with 3 ml containing a 1:1 mixture of 1.2% oxoid agar
247 and 2X DMEM (Gibco, Carlsbad, CA) with 10% (vol/vol) FBS and 2% (vol/vol)
248 penicillin/streptomycin. Cells were incubated at 37°C in 5% CO_2 for four days for plaque
249 development. Cell monolayers then were stained with 3 mL of overlay containing a 1:1 mixture
250 of 1.2% oxoid agar and 2X DMEM with 2% (vol/vol) FBS, 2% (vol/vol) penicillin/streptomycin,
251 and 0.33% neutral red (Gibco). Cells were incubated overnight at 37°C and plaques were
252 counted.

253

254 *Immunophenotyping*

255 The amount of activated/proliferating NK cells were quantified using a modified version of our
256 protocol detailed step-by step in OMIP-28[24]. Briefly 0.1 mL of EDTA-anticoagulated whole blood
257 samples were incubated for 15 min at room temperature in the presence of a mastermix of
258 antibodies against CD45 (clone D058-1283, Brilliant Violet 786 conjugate), CD3 (clone SP34-2
259 Alexa Fluor 700 conjugate), CD8 (clone SK2, Brilliant Violet 510), NKG2A/C (clone Z199, PE-
260 Cy7 conjugate), CD16 (clone 3G8, Pacific Blue conjugate), CD69 (clone TP1.55.3, ECD
261 conjugate), HLA-DR (clone 1D11, Brilliant Violet 650 conjugate), CD4 (clone SK3, Brilliant Violet
262 711 conjugate), CCR7 (clone 150503, Fluorescein conjugate), CD28 (clone CD28.2, PE
263 conjugate), and CD95 (clone DX2, PE-Cy5 conjugate) antigens. All antibodies were obtained
264 from BD BioSciences, except the NKG2A/C-specific antibody, which was purchased from
265 Beckman Coulter and the CCR7 antibody that was purchased from R&D Systems. Red blood
266 cells were lysed using BD Pharm Lyse, after which they were washed twice in media and fixed
267 with 0.125 ml of 2% paraformaldehyde for 15 min. After an additional wash the cells were
268 permeabilized using Life Technology's Bulk Permeabilization Reagent. The cells were stained
269 for 15 min. against Ki-67 (clone B56, Alexa Fluor 647 conjugate) while the permeabilizer was
270 present. The cells were then washed twice in media and resuspended in 0.125 ml of 2%
271 paraformaldehyde until they were run on a BD LSRII Flow Cytometer. Flow data were analyzed
272 using Flowjo version 9.8.2.

273

274 *Plasmablast detection*

275 Peripheral blood mononuclear cells (PBMCs) isolated from three ZIKV-infected rhesus monkeys
276 at 3, 7, 11, and 14 dpi were stained with the following panel of fluorescently labeled antibodies
277 (Abs) specific for the following surface markers: CD20 FITC (L27), CD80 PE(L307.4), CD123

278 PE-Cy7(7G3), CD3 APC-Cy7 (SP34-2), IgG BV605(G18-145) (all from BD Biosciences, San
279 Jose, CA), CD14 AF700 (M5E2), CD11c BV421 (3.9), CD16 BV570 (3G8), CD27 BV650(O323)
280 (all from BioLegend, San Diego, CA), IgD AF647 (polyclonal)(Southern Biotech, Birmingham,
281 AL), and HLA-DR PE-TxRed (TÜ36) (Invitrogen, Carlsbad, CA). LIVE/DEAD Fixable Aqua Dead
282 Cell Stain Kit (Invitrogen, Carlsbad, CA) was used to discriminate live cells. Briefly, cells were
283 resuspended in 1X PBS/1%BSA and stained with the full panel of surface Abs for 30 min in the
284 dark at 4°C, washed once with 1X PBS, stained for 30 min with LIVE/DEAD Fixable Aqua Dead
285 Cell Stain Kit in the dark at 4°C, washed once with 1X PBS, washed again with 1X
286 PBS/1%BSA, and resuspended in 2% PFA Solution. Stained PBMCs were acquired on a LSRII
287 Flow Analyzer (BD Biosciences, San Jose, CA) and the data was analyzed using FlowJo
288 software v9.7.6 (TreeStar, Ashland, OR). Plasmablasts were defined similarly to the method
289 previously described[23] excluding lineage cells (CD14+, CD16+, CD3+, CD20+, CD11c+,
290 CD123+), and selecting CD80+ and HLA-DR+ cells (known to be expressed on rhesus
291 plasmablasts and their human counterpart[25]).
292
293 *Estimation of plasma viremia doubling time*
294 The doubling time of plasma viremia was estimated in R version 3.2.3 (The R Foundation for
295 Statistical Computing, http://www.R-project.org). For each animal, the slope of the linear portion
296 of the line (between 1 and 2 dpi for the animals treated with $1x10^6$ and $1x10^5$ PFU and between
297 1, 2, and 3 dpi for the animal treated with $1x10^4$ PFU) was generated by plotting the log of the
298 plasma viral loads. The linear portion represents the exponential growth phase and has been
299 used to estimate doubling time in other systems[26]. The slopes were then used in the equation:
300 log(2)/slope. Each result was then multiplied by 24 hours to produce a simple estimate of
301 doubling time in hours.
302

303 *CBC and blood chemistry panels*

304 CBCs were performed on EDTA-anticoagulated whole blood samples on a Sysmex XS-1000i
305 automated hematology analyzer (Sysmex Corporation, Kobe, Japan). Blood smears were
306 prepared and stained with Wright-Giemsa stain (Wescor Aerospray Hematology Slide Stainer;
307 Wescor Inc, Logan, UT). Manual slide evaluations were performed on samples as appropriate
308 when laboratory-defined criteria were met (including the presence of increased total white blood
309 cell counts, increased monocyte, eosinophil, and basophil percentages, decreased hemoglobin,
310 hematocrit, and platelet values, and unreported automated differential values). Individuals
311 performing manual slide evaluations screened both white blood cells (WBC) and red blood cells
312 (RBC) for cellular maturity, toxic change, and morphologic abnormalities.

313 Whole blood was collected into serum separator tubes (Becton, Dickinson and
314 Company, Franklin Lakes, NJ) for blood chemistry analysis and processed per manufacturer's
315 instructions. Blood chemistry panels were performed on the serum using a Cobas 6000
316 analyzer (Roche Diagnostics, Risch-Rotkreuz, Switzerland). Results from CBC and blood
317 chemistry panels were reported with species, age, and sex-specific reference ranges.

318

319 *Zika virus deep sequencing from plasma*

320 A vial of the same ZIKV strain H/PF/2013 virus stock that infected macaques was deep
321 sequenced by preparing libraries of fragmented double-stranded cDNA using methods similar to
322 those previously described[27]. Briefly, the sample was centrifuged at 5000 rcf for 5 min. The
323 supernatant was then filtered through a 0.45-um filter. The Qiagen QiAmp Minelute viral RNA
324 isolation kit (omitting carrier RNA) was used to isolate vRNA. The eluted RNA was then treated
325 with DNAse I. Double stranded DNA was prepared with the Superscript double stranded cDNA
326 synthesis kit (Invitrogen) and priming with random hexamers. Agencourt Ampure XP beads
327 were used to purify double stranded DNA. The purified DNA was fragmented with the Nextera
328 XT kit (Illumina), tagged with Illumina-compatible primers, and then purified with Agencourt

329 Ampure XP beads. Purified libraries were then sequenced with 2 x 300 bp kits on an Illumina
330 MiSeq.
331 Zika virus samples isolated from animals were PCR amplified to create a series of five
332 overlapping amplicons that span the entire viral polyprotein, as described previously for other
333 RNA viruses[28]. Briefly, vRNA was isolated using the Qiagen QiAmp Minelute viral RNA isolation
334 kit, according to manufacturer's protocol (Qiagen). The following primer pairs were used to
335 generate viral cDNA amplicons using the Superscript III One-step RT-PCR kit (Invitrogen) and
336 including MgSO4:
337 ZFP-1F: GCGACAGTTCGAGTTTGAAGCG; ZFP-1R: ATCCAAAGTCCCAGGCTGTG;
338 ZFP-2F: AGATCCCGGCTGAAACACTG; ZFP-2R: CCCATGTGATGTCACCTGCT;
339 ZFP-3F: TACTCACAGCTGTTGGCCTG; ZFP-3R: CACCTCGGTTTGAGCACTCT;
340 ZFP-4F: TGTTTGGCTGGCCTATCAGG; ZFP-4R: CTGCGGATCCTTTCAATGCG;
341 ZFP-5F: TATGGGGGAGGACTGGTCAG; ZFP-5R: ACTAGCAGGCCTGACAACAC.
342 The following cycling conditions were used: 55°C for 30 min; 94°C 2 min; 35 cycles of the
343 following: 94°C 15 sec, 56°C 30 sec, and 68°C 3.5 min; 68°C 10 min. Viral cDNA amplicons
344 were size selected by agarose gel electrophoresis and then purified using the Qiagen MinElute
345 Gel extraction kit. Purified PCR products were pooled and then ~1ng of DNA was fragmented
346 using the Nextera XT kit (Illumina), tagged with Illumina-compatible primers, and then purified
347 with Agencourt Ampure XP beads. Purified libraries were then sequenced with 2 x 300bp kits on
348 an Illumina MiSeq.
349 Sequences were analyzed using a workflow (https://bitbucket.org/dhoconno/zequencer)
350 implemented in Geneious Pro (Biomatters, Ltd.). Briefly, duplicate reads were initially removed
351 with the BBMap v35.82 dedupe tool (https://sourceforge.net/projects/bbmap/) using a kmer seed
352 length of 31 bp and allowing zero edits or substitutions. Non-duplicate reads were quality
353 trimmed with BBDuk v35.82 to remove Truseq, Nextera, and PhiX adapters from both the left
354 and right ends of sequences. Regions with low quality sequences (average quality < 20) were

355 removed from both ends of remaining sequence reads, and only reads longer than than 150 bp
356 are retained. BBMap v35.82 was used to map these reads to the ZIKV strain H/PF/2013
357 Genbank reference sequence (KJ776791) in local alignment mode using the normal sensitivity
358 preset. The Geneious Pro 9.1.2 variant caller is used to detect and annotate variants. Variants
359 are called that fit the following conditions: present in >=5% of the mapped reads, have a
360 minimum p-value of 10e-60, and a minimum strand bias of 10e-5. Areas with low coverage
361 (<20x) are annotated.
362
363 *Calculating nucleotide diversity*
364 Synonymous (πS) and Nonsynonymous (πN) nucleotide diversity were calculated for each
365 coding region using Popoolation version 1.2.2[29]reference-based mappings were exported from
366 Geneious as bam files, which were converted to sorted pileup files using SAMtools[30]. πN and
367 πS estimates were calculated for each coding region in the genome using the Syn-
368 nonsyn-at-position.pl script. πS > πN suggests that purifying selection is acting to remove new
369 variation, πN > πS suggests that diversifying selection is favoring new mutations, and πN = πS
370 indicates no strong selection. To reduce the effects of uneven coverage across sites, pileup files
371 were subsampled such that every position was covered by exactly 1000x using the subsample-
372 pileup.pl script in Popoolation. Regions in which coverage was <1000x were excluded from the
373 analysis. πN and πS estimates were then calculated for each coding region in the genome
374 using the Syn-nonsyn-at-position.pl script. Corrections were disabled.
375
376 **References**
377 1. Brasil, P. et al. Zika Virus Infection in Pregnant Women in Rio de Janeiro - Preliminary
378 Report. *N Engl J Med* (2016).
379 2. Cao-Lormeau, V. M. et al. Guillain-Barré Syndrome outbreak associated with Zika virus
380 infection in French Polynesia: a case-control study. *Lancet* (2016).

381 3. Calvet, G. et al. Detection and sequencing of Zika virus from amniotic fluid of fetuses with
382 microcephaly in Brazil: a case study. *Lancet Infect Dis* (2016).
383 4. Carteaux, G. et al. Zika Virus Associated with Meningoencephalitis. *N Engl J Med* (2016).
384 5. Haddow, A. D. et al. Genetic characterization of Zika virus strains: geographic expansion
385 of the Asian lineage. *PLoS Negl Trop Dis* **6**, e1477 (2012).
386 6. Marchette, N. J., Garcia, R. & Rudnick, A. Isolation of Zika virus from Aedes aegypti
387 mosquitoes in Malaysia. *Am J Trop Med Hyg* **18**, 411-415 (1969).
388 7. de M Campos, R. et al. Prolonged detection of Zika virus RNA in urine samples during the
389 ongoing Zika virus epidemic in Brazil. *J Clin Virol* **77**, 69-70 (2016).
390 8. Mansuy, J. M. et al. Zika virus: high infectious viral load in semen, a new sexually
391 transmitted pathogen. *Lancet Infect Dis* (2016).
392 9. Musso, D. et al. Detection of Zika virus in saliva. *J Clin Virol* **68**, 53-55 (2015).
393 10. Dupont-Rouzeyrol, M., Biron, A., O'Connor, O., Huguon, E. & Descloux, E. Infectious Zika
394 viral particles in breastmilk. *Lancet* (2016).
395 11. Musso, D. et al. Potential sexual transmission of Zika virus. *Emerg Infect Dis* **21**, 359-361
396 (2015).
397 12. Foy, B. D. et al. Probable non-vector-borne transmission of Zika virus, Colorado, USA.
398 *Emerg Infect Dis* **17**, 880-882 (2011).
399 13. Cunha, M. S. et al. First Complete Genome Sequence of Zika Virus (Flaviviridae,
400 Flavivirus) from an Autochthonous Transmission in Brazil. *Genome Announc* **4**, (2016).
401 14. DICK, G. W., KITCHEN, S. F. & HADDOW, A. J. Zika virus. I. Isolations and serological
402 specificity. *Trans R Soc Trop Med Hyg* **46**, 509-520 (1952).
403 15. Styer, L. M. et al. Mosquitoes inoculate high doses of West Nile virus as they probe and
404 feed on live hosts. *PLoS Pathog* **3**, 1262-1270 (2007).
405 16. Osorio, J. E. et al. Efficacy of a tetravalent chimeric dengue vaccine (DENVax) in
406 Cynomolgus macaques. *Am J Trop Med Hyg* **84**, 978-987 (2011).

407 17. Lanciotti, R. S. et al. Genetic and serologic properties of Zika virus associated with an
408 epidemic, Yap State, Micronesia, 2007. *Emerg Infect Dis* **14**, 1232-1239 (2008).
409 18. Lindenbach, B. D. & Rice, C. M. Molecular biology of flaviviruses. *Adv Virus Res* **59**, 23-61
410 (2003).
411 19. Muller, D. A. & Young, P. R. The flavivirus NS1 protein: molecular and structural biology,
412 immunology, role in pathogenesis and application as a diagnostic biomarker. *Antiviral Res*
413 **98**, 192-208 (2013).
414 20. Avirutnan, P. et al. Antagonism of the complement component C4 by flavivirus
415 nonstructural protein NS1. *J Exp Med* **207**, 793-806 (2010).
416 21. Tappe, D. et al. Acute Zika virus infection after travel to Malaysian Borneo, September
417 2014. *Emerg Infect Dis* **21**, 911-913 (2015).
418 22. Zammarchi, L. et al. Zika virus infections imported to Italy: clinical, immunological and
419 virological findings, and public health implications. *J Clin Virol* **63**, 32-35 (2015).
420 23. Silveira, E. L. et al. Vaccine-induced plasmablast responses in rhesus macaques:
421 phenotypic characterization and a source for generating antigen-specific monoclonal
422 antibodies. *J Immunol Methods* **416**, 69-83 (2015).
423

424 **References from methods section only**

425 24. Pomplun, N., Weisgrau, K. L., Evans, D. T. & Rakasz, E. G. OMIP-028: activation panel
426 for Rhesus macaque NK cell subsets. *Cytometry A* **87**, 890-893 (2015).
427 25. Wrammert, J. et al. Rapid cloning of high-affinity human monoclonal antibodies against
428 influenza virus. *Nature* **453**, 667-671 (2008).
429 26. Staprans, S. I. et al. Simian immunodeficiency virus disease course is predicted by the
430 extent of virus replication during primary infection. *J Virol* **73**, 4829-4839 (1999).
431 27. Lauck, M. et al. Discovery and full genome characterization of two highly divergent simian
432 immunodeficiency viruses infecting black-and-white colobus monkeys (Colobus guereza)

433 in Kibale National Park, Uganda. *Retrovirology* **10**, 107 (2013).
434 28. Gellerup, D. D. et al. Conditional Immune Escape during Chronic Simian
435 Immunodeficiency Virus Infection. *J Virol* **90**, 545-552 (2015).
436 29. Kofler, R. et al. PoPoolation: a toolbox for population genetic analysis of next generation
437 sequencing data from pooled individuals. *PLoS One* **6**, e15925 (2011).
438 30. Li, H. et al. The Sequence Alignment/Map format and SAMtools. *Bioinformatics* **25**, 2078-
439 2079 (2009).
440
441 **Supplementary Information** is linked to the online version of the paper at
442 www.nature.com/nature.
443
444 **Acknowledgements** We thank the Veterinary, animal care, Scientific Protocol Implementation,
445 and the Pathology staff at the Wisconsin National Primate Research Center (WNPRC) for their
446 contribution to this study. We thank the DHHS/PHS/NIH (R01AI116382-01A1) and
447 (DP2HD075699) for funding. We also thank the P51OD011106 awarded to the WNPRC,
448 Madison-Wisconsin. This research was conducted in part at a facility constructed with support
449 from Research Facilities Improvement Program grants RR15459-01 and RR020141-01. The
450 publication's contents are solely the responsibility of the authors and do not necessarily
451 represent the official views of NCRR or NIH.
452
453 **Author contributions** D.H.O., T.C.F., J.E.O., M.T.A., E.M., T.G.G. and D.M.D. designed the
454 experiments. D.H.O., D.M.D., M.T.A., E. M., T.C.F., and L.H.M. drafted the manuscript. M.T.A.,
455 and J.E.O. provided and prepared viral stocks and performed plaque assays. A.M.W., G.L-B.,
456 and T.C.F. developed and performed viral load assays. K.L.W. and E.G.R. performed
457 immunophenotyping assays. M.S.M., M.E.B., M.N.R., C.M.N., and D.M.D. coordinated and
458 processed macaque samples for distribution. D.D.G., S.L.O., and D.M.D. designed and

459 performed the sequencing experiments. L.H.M. and T.C.F. performed nucleotide diversity
460 calculations. J.P., N.S-D., H.A.S., S.C., coordinated the macaque infections, sampling, and
461 performed blood chemistries and CBC analysis. J.A.E., M.A.M., and S.R.P. performed the
462 plasmablast experiments.
463
464 **Author information:** Sequences are pending deposition into the Sequence Read Archive at
465 NCBI. The bioSample accession number is SAMN04589872. All data from these studies are
466 available at zika.labkey.com. Reprints and permissions information is available at
467 www.nature.com/reprints. The authors declare no competing interests. Correspondence and
468 requests for materials should be addressed to dhoconno@wisc.edu.
469
470 **Figure Legends**
471 **Figure 1. Study design and ZIKV viral load from rhesus macaque fluids.** a. ZIKV, strain
472 H/FP2013 from the European virus archive (Genbank: KJ776791) was inoculated onto C6/36
473 mosquito cells to generate the stock Zika virus/H.sapiens-tc/FRA/2013/FrenchPolynesia-
474 01_v1c1. Doses administered subcutaneously per animal are shown. b. Viral loads were
475 measured in plasma, urine, saliva and cerebral spinal fluid for each animal through 28 dpi. CSF
476 was collected on days 4 and 14. All animals were negative on day 14.
477
478 **Figure 2. Genetic diversity of the challenge stock and virus isolated from animals.** a. The
479 ZIKV challenge stock was deep sequenced from all three animals. Nucleotide sites where at
480 least 5% of sequences obtained from the challenge stock are different from the Genbank
481 sequence are shown. b. The plasma virus of each animal from 4 dpi was deep sequenced.
482 Non-synonymous variants present in the challenge stock relative to the Genbank consensus
483 sequence are shown in black in all three plots; synonymous variants are shown in grey. Variants
484 detected relative to the challenge stock in each animal are colored based on animal.

485 Non-synonymous variants are shown with dark colored markers, while synonymous variants are
486 shown in a lighter shade. Changes found in both the stock and the animals are connected with a
487 line. c. Deep sequence data from all 3 animals on day 4 post-infection were used to calculate
488 measures of synonymous (πS) and nonsynonymous (πN) nucleotide diversity for each coding
489 region in the genome. The πN/πS ratio for each gene is shown with color corresponding to
490 animal. The capsid, propeptide and membrane coding regions in animal 393422 were excluded
491 from the analysis due to coverage <1000x.
492
493 **Figure 3. Immune cell expansion following ZIKV infection.** Expansion of Ki-67+ (activated)
494 CD4+, CD8+ and NK cells were measured daily for 11 days and then every 3 days for each
495 animal. Total number of activated cells per microliter of blood are plotted for each animal for
496 each cell type over time. The inset of each graph shows the total number of plasmablast cells
497 found in PBMCs collected at 3, 7, 11 and 14 dpi for each animal. Viral load is graphed over the
498 columns as a reference.
499
500 **Extended Data Figure 1. Complete blood counts and chemistries for macaques infected**
501 **with ZIKV.** Animals were infected with different doses of ZIKV as described in panel a.
502 Chemistries (AST in b; ALT in c; CK in d) were measured prior to infection and on 2, 5, and 11
503 dpi. Complete blood counts (WBC in e; % lymphocytes in f; RBC in g; platelets in h) were
504 measured prior to infection, daily for 11 days after infection and then every 3 days until 28 dpi.
505
506 **Extended Data Figure 2. Infection with African lineage ZIKV.** ZIKV strain MR766 (GenBank:
507 LC002520), originally isolated from a sentinel rhesus macaque on 20 April 1947 in Zika Forest,
508 Entebbe, Uganda with 149 suckling mouse brain passages and two rounds of amplification on
509 Vero cells, was obtained from Brandy Russell (CDC, Ft. Collins, CO). Virus stocks were

510 prepared by inoculation onto a confluent monolayer of C6/36 mosquito cells to generate the
511 stock Zika virus/R.macaque-tc/UGA/1947/MR766-3329. The viral loads for the first seven dpi
512 are shown relative to the viral loads of animals receiving the same dose of Asian lineage ZIKV.
513
514 **Extended Data Figure 3. Efficiency of qRT-PCR on different templates with different**
515 **primers.** The region of NS1 targeted by the Lanciotti et al. (2008) QRT-PCR assay is not
516 completely conserved between Asian and African lineage Zika viruses. We therefore introduced
517 ambiguous bases at sites in the primers and probe that varied between lineages. To determine
518 whether the modified oligos amplify and detect both African and Asian lineage viruses with
519 equal efficiency we compared tenfold dilution series of a Ugandan Zika virus, French Polynesian
520 Zika virus and our in-vitro transcribed RNA standard in this assay (which we term “universal”)
521 with the same samples amplified with the sequence-specific (Lanciotti) primers and probe. Both
522 assays amplified samples with essentially equivalent efficiencies. (The slopes of the lines are
523 1.011, 1.012 and 1.020 respectively). Not surprisingly, the concentration of the Ugandan virus
524 is roughly 2-fold higher when measured with the universal assay than when measured with the
525 original Lanciotti assay. The computed concentration of the French Polynesian virus is the same
526 regardless of assay used to quantify the virus.
527
528

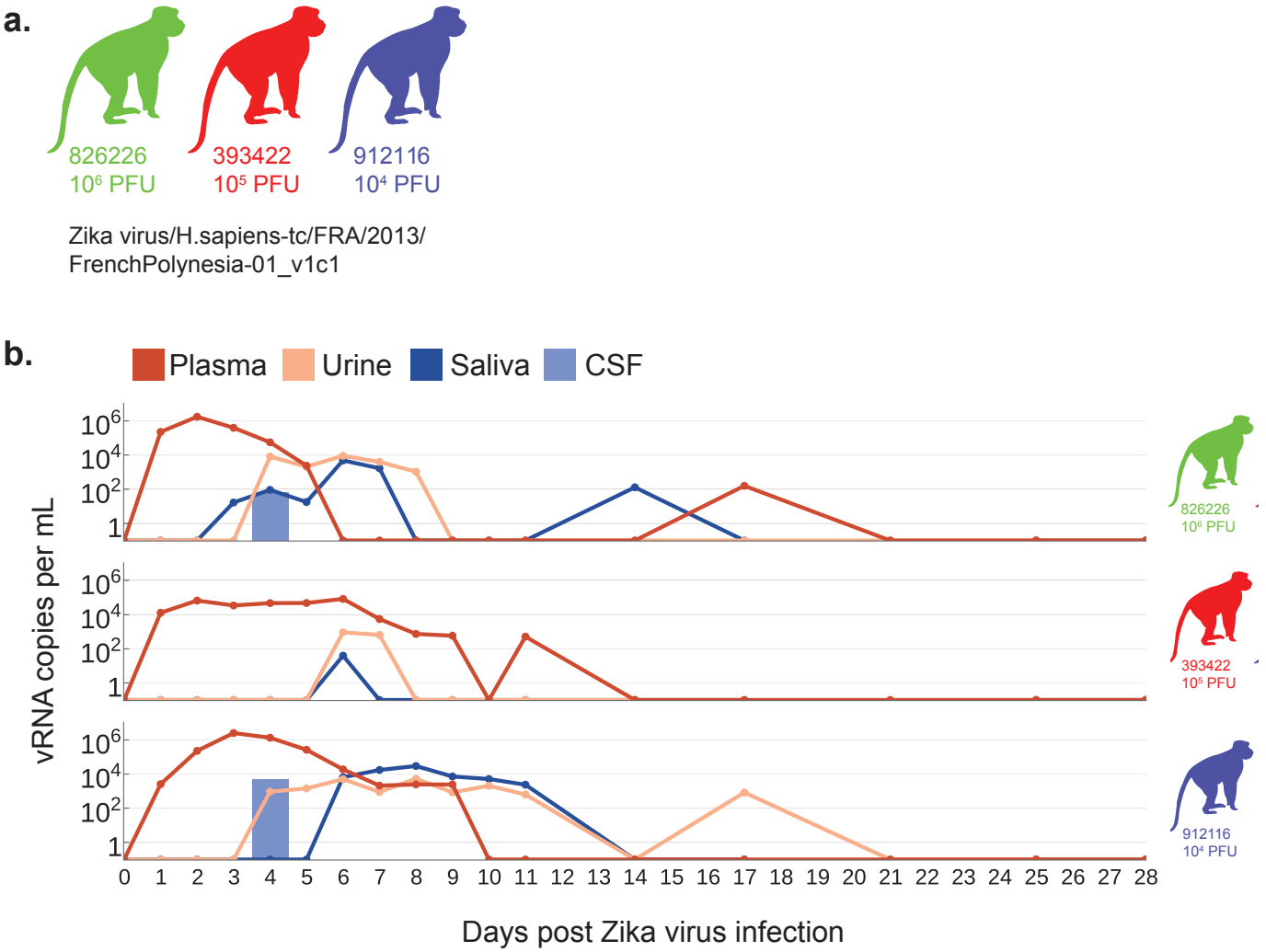

Figure 1. Study design and ZIKV viral load from rhesus macaque fluids. a. ZIKV, strain H/FP2013 from the European virus archive (Genbank: KJ776791) was inoculated onto C6/36 mosquito cells to generate the stock Zika virus/H.sapiens-tc/FRA/2013/FrenchPolynesia-01_v1c1. Doses administered subcutaneously per animal are shown. b. Viral loads were measured from plasma, urine, saliva or cerebral spinal fluid for each animal through 28 dpi. CSF was collected on days 4 and 14. All animals were negative on day 14.

a.

Site relative to KJ776791	Change	Amino Acid Change	Codon Change	Protein Effect	Variant Frequency
801	T -> C	F->L	UUC->CUC	Substitution	17.9%
2318	C -> T		CUC->CUT	None	18.7%
2863	T -> C	L->P	CUC->CCC	Substitution	7.7%
3223	A -> T	K->I	AAA->ATA	Substitution	10.5%
3475	T -> C	M->T	AUG->ACG	Substitution	7.9%
3740	C -> T		GUC->GUT	None	11.1%
3835	C -> T	A->V	GCG->GTG	Substitution	15.8%
4242	G -> C	E->Q	GAG->CAG	Substitution	40.9%

b.

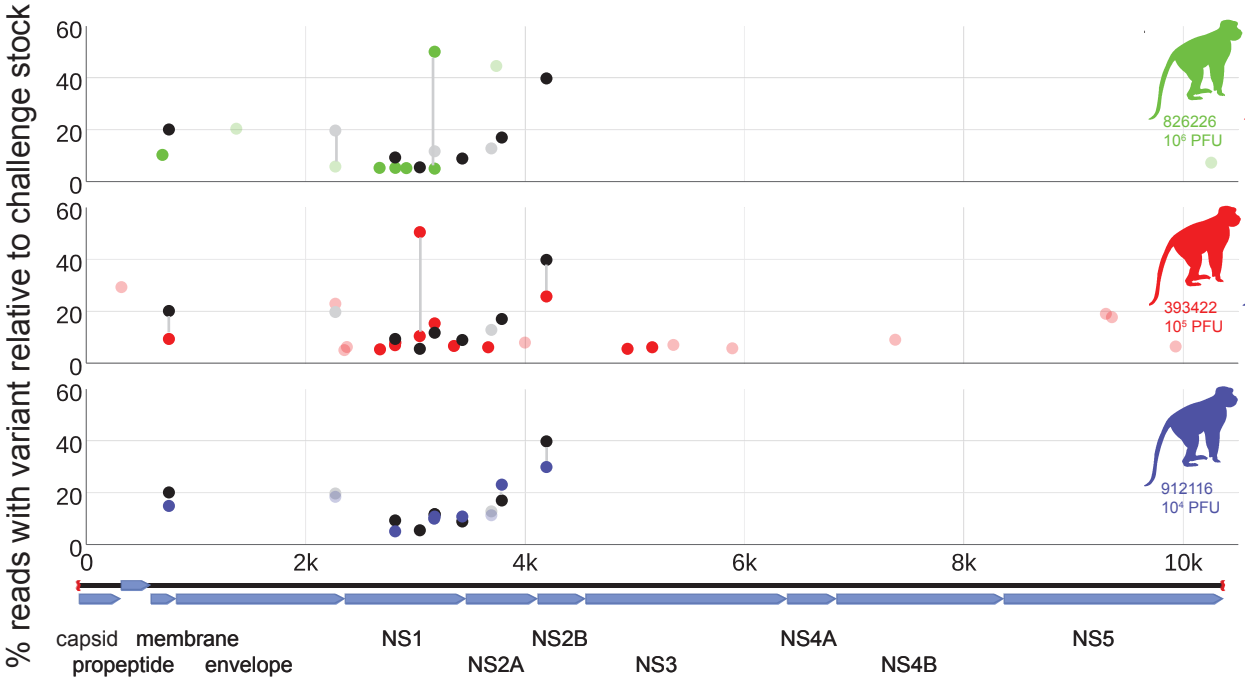

c.

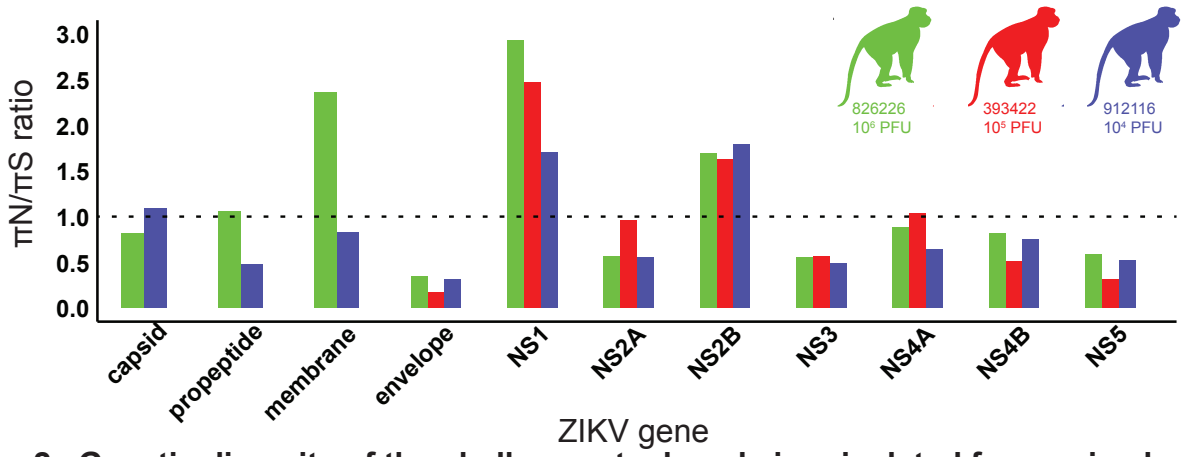

Figure 2. Genetic diversity of the challenge stock and virus isolated from animals. a. The ZIKV challenge stock was deep sequenced from all three animals. Nucleotide sites where at least 5% of sequences obtained from the challenge stock are different from the Genbank sequence are shown. b. The plasma virus of each animal from 4 dpi was deep sequenced. Non-synonymous variants present in the challenge stock relative to the Genbank consensus sequence are shown in black in all three plots; synonymous variants are shown in grey.

Variants detected relative to the challenge stock in each animal are colored based on animal. Nonsynonymous variants are shown with dark colored markers, while synonymous variants are shown in a lighter shade. Changes found in both the stock and the animals are connected with a line. c. Deep sequence data from all 3 animals on day 4 postinfection were used to calculate measures of synonymous (πS) and nonsynonymous (πN) nucleotide diversity for each coding region in the genome. The $\pi N/\pi S$ ratio for each gene is shown with color corresponding to animal. The capsid, propeptide and membrane coding regions in animal 393422 were excluded from the analysis due to coverage <1000x.

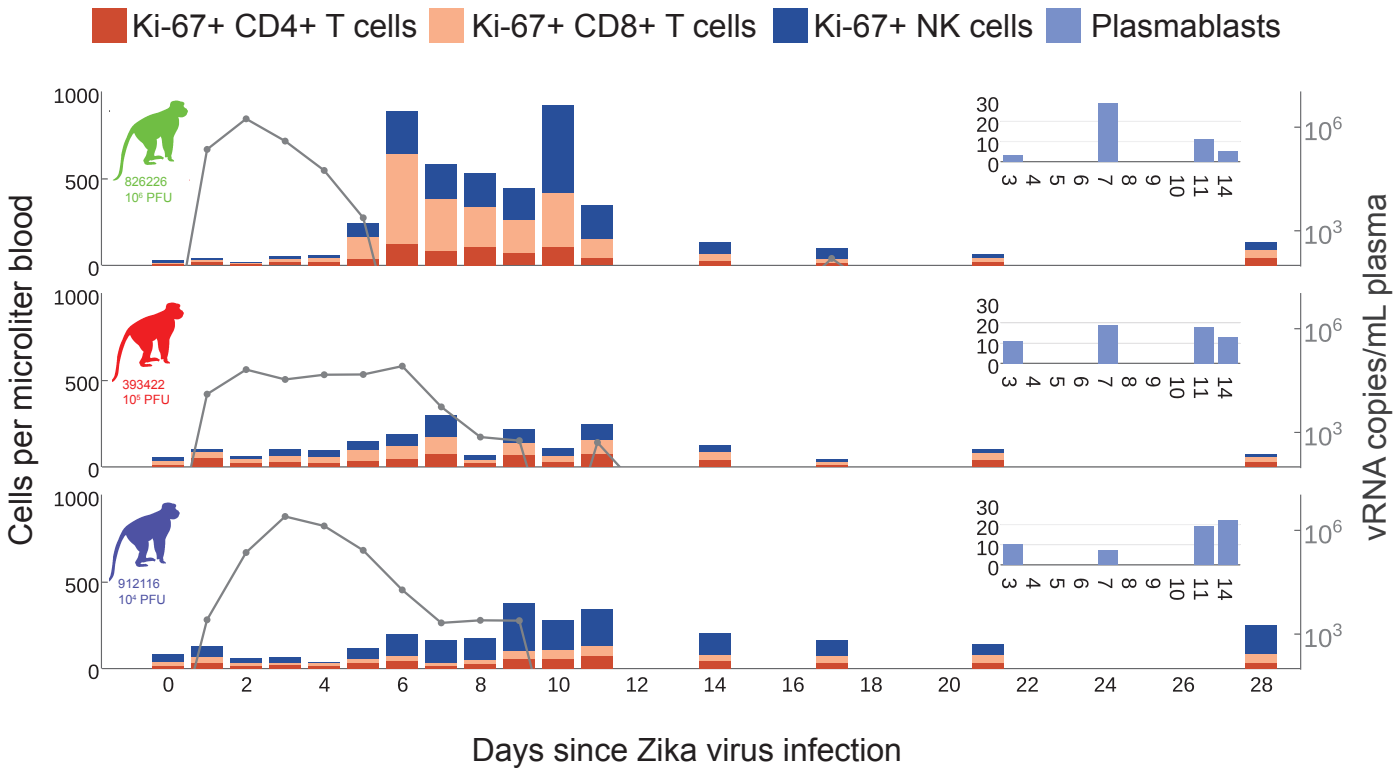

Figure 3. Immune cell expansion following ZIKV infection. Expansion of Ki-67+ (activated) CD4+, CD8+ and NK cells were measured daily for 11 days and then every 3 days for each animal. Total numbers of activated cells per microliter of blood are plotted for each animal for each cell type over time. The inset of each graph shows the total number of plasmablast cells found in PBMCs collected at days 3, 7, 11 and 14 dpi for each animal. Viral load is graphed over the columns as a reference.

a.

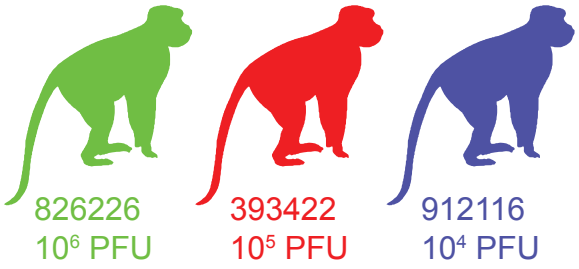
826226
10^6 PFU
393422
10^5 PFU
912116
10^4 PFU

b.

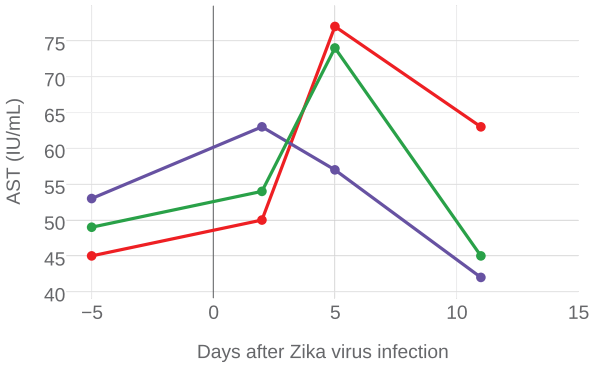
AST (IU/mL)
75
70
65
60
55
50
45
40
−5
0
5
10
15
Days after Zika virus infection

c.

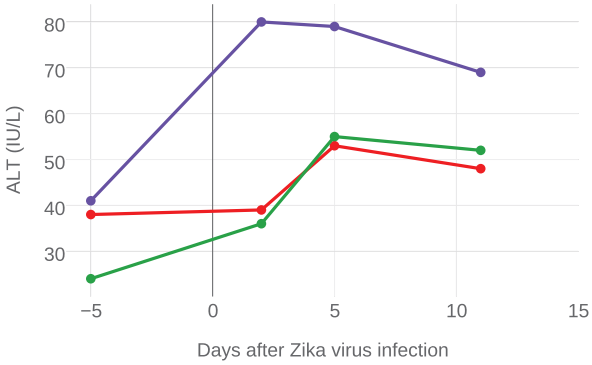
ALT (IU/L)
80
70
60
50
40
30
−5
0
5
10
15
Days after Zika virus infection

d.

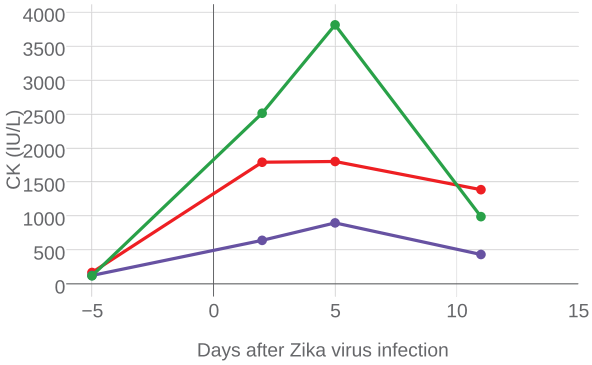
CK (IU/L)
4000
3500
3000
2500
2000
1500
1000
500
0
−5
0
5
10
15
Days after Zika virus infection

e.

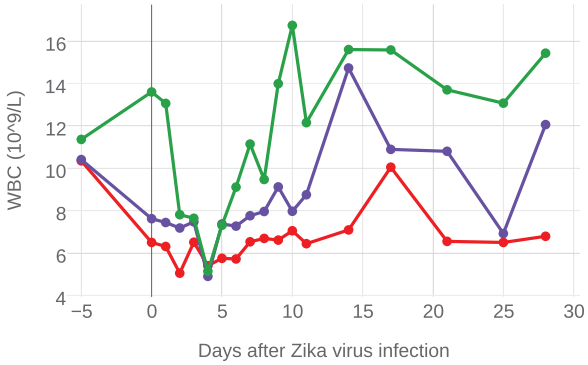
WBC (10^9/L)
16
14
12
10
8
6
4
−5
0
5
10
15
20
25
30
Days after Zika virus infection

f.

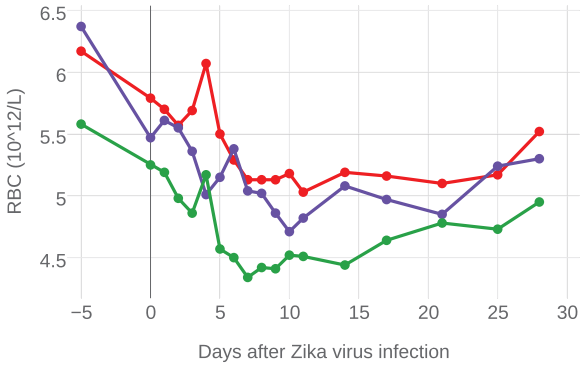
RBC (10^12/L)
6.5
6
5.5
5
4.5
−5
0
5
10
15
20
25
30
Days after Zika virus infection

g.

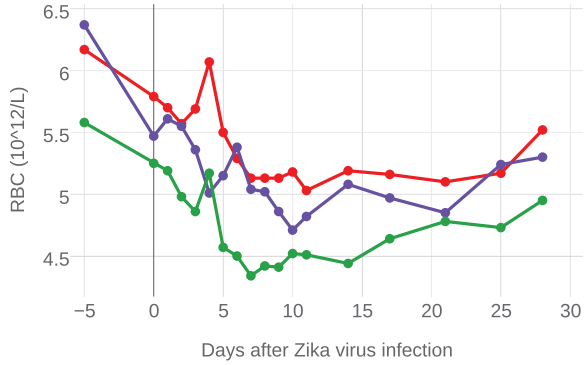
RBC (10^12/L)
6.5
6
5.5
5
4.5
−5
0
5
10
15
20
25
30
Days after Zika virus infection

h.

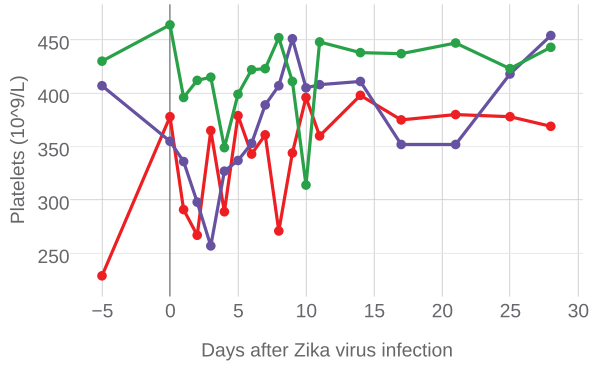
Platelets (10^9/L)
450
400
350
300
250
−5
0
5
10
15
20
25
30
Days after Zika virus infection

Extended Data Figure 1. Complete blood counts and chemistries for macaques infected with ZIKV. Animals were infected with different doses of ZIKV as described in panel a. Chemistries (AST in b; ALT in c; CK in d) were measured prior to infection and on 2, 5, and 11 dpi. Complete blood counts (WBC in e; % lymphocytes in f; RBC in g; platelets in h) were measured prior to infection, daily for 11 days after infection and then every 3 days until 28 dpi.

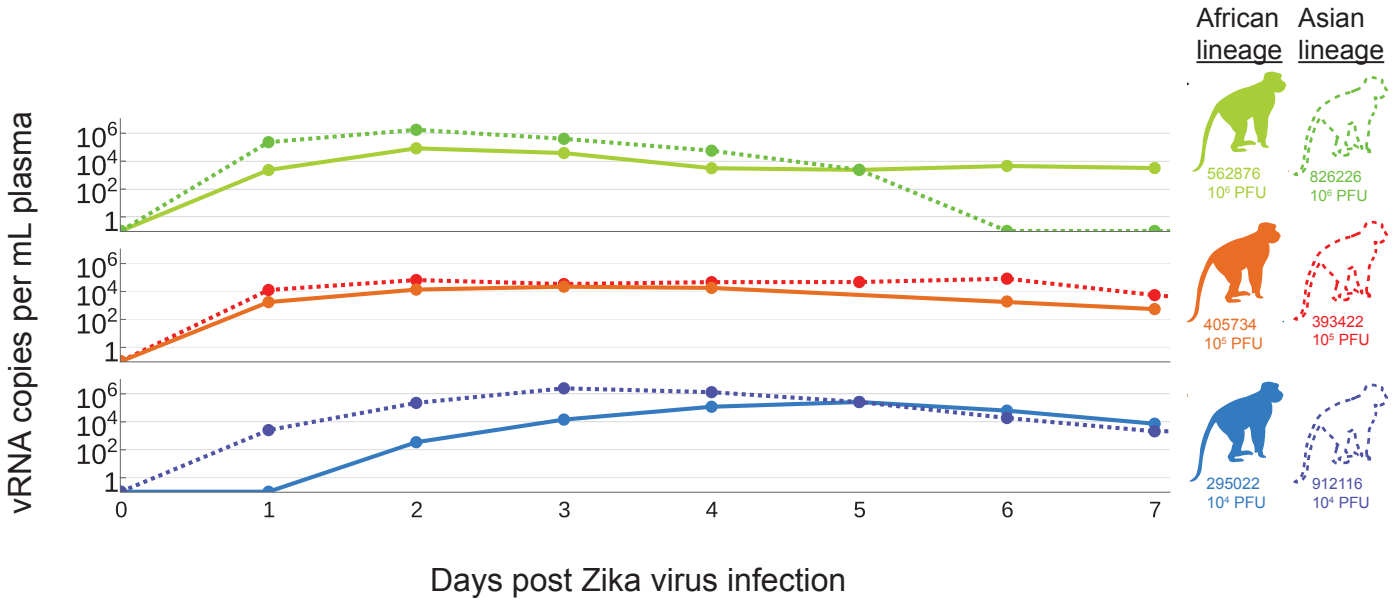

Extended Data Figure 2. Infection with African lineage ZIKV. ZIKV strain MR766 (GenBank: LC002520), originally isolated from a sentinel rhesus macaque on 20 April 1947 in Zika Forest, Entebbe, Uganda with 149 suckling mouse brain passages and two rounds of amplification on Vero cells, was obtained from Brandy Russell (CDC, Ft. Collins, CO). Virus stocks were prepared by inoculation onto a confluent monolayer of C6/36 mosquito cells to generate the stock Zika virus/R.macaque-tc/UGA/1947/MR766-3329. The viral loads for the first seven dpi are shown relative to the viral loads of animals receiving the same dose of Asian lineage ZIKV.

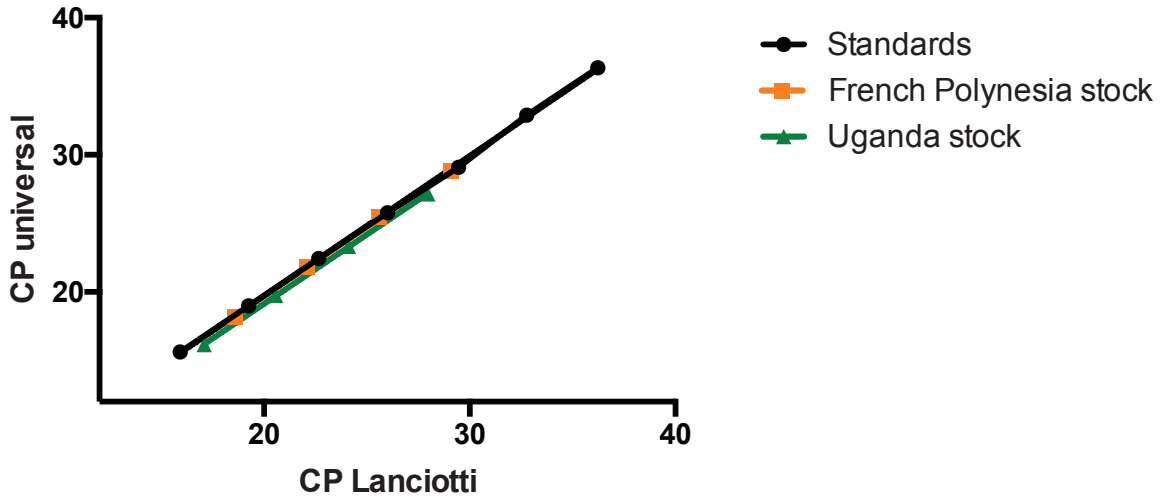

Extended Data Figure 3. Efficiency of qRT-PCR on different templates with different primers. The region of NS1 targeted by the Lanciotti et al. (2008) QRT-PCR assay is not completely conserved between Asian and African lineage Zika viruses. We therefore introduced ambiguous bases at sites in the primers and probe that varied between lineages. To determine whether the modified oligos amplify and detect both African and Asian lineage viruses with equal efficiency we compared tenfold dilution series of a Ugandan Zika virus, French Polynesian Zika virus and our in-vitro transcribed RNA standard in this assay (which we term "universal") with the same samples amplified with the sequence-specific (Lanciotti) primers and probe. Both assays amplified samples with essentially equivalent efficiencies. (The slopes of the lines are 1.011, 1.012 and 1.020 respectively). Not surprisingly, the concentration of the Ugandan virus is roughly 2-fold higher when measured with the universal assay than when measured with the original Lanciotti assay. The computed concentration of the French Polynesian virus is the same regardless of assay used to quantify the virus.